

Model-Based Assessment of Cardiovascular Autonomic Control in Children with Obstructive Sleep Apnea

Jarree Chaicham, PhD¹; Zheng Lin, PhD¹; Maida L. Chen, MD²; Sally L.D. Ward, MD³; Thomas Keens, MD³; Michael C. K. Khoo, PhD¹

Departments of ¹Biomedical Engineering and ²Medicine, University of Southern California, Los Angeles, CA; ³Department of Pediatric Pulmonology, Children's Hospital Los Angeles, Los Angeles, CA

Study Objectives: To quantitatively assess daytime autonomic cardiovascular control in pediatric subjects with and without obstructive sleep apnea syndrome (OSAS).

Design: Respiration, R-R intervals, and noninvasive continuous blood pressure were monitored in awake subjects in the supine and standing postures, as well as during cold face stimulation.

Setting: Sleep disorders laboratory in a hospital setting.

Participants: Ten pediatric patients (age 11.4 ± 3.6 years) with moderate to severe OSAS (obstructive apnea-hypopnea index = 21.0 ± 6.6 /h) before treatment and 10 age-matched normal control subjects (age 11.5 ± 3.7 years).

Measurements and Results: Spectral analysis of heart rate variability revealed that high-frequency power was similar and the ratio of low- to high-frequency power was lower in subjects with OSAS vs control subjects. The closed-loop minimal model allowed heart rate variability to be partitioned into a component mediated by respiratory-cardiac coupling and a baroreflex component, whereas blood pressure variability was

assumed to result from the direct effects of respiration and fluctuations in cardiac output. Baroreflex gain was lower in subjects with OSAS vs control subjects. Under orthostatic stress, respiratory-cardiac coupling gain decreased in both subject groups, but baroreflex gain decreased only in controls. The model was extended to incorporate time-varying parameter changes for analysis of the data collected during cold face stimulation: cardiac output gain increased in controls but remained unchanged in OSAS.

Conclusions: Our findings suggest that vagal modulation of the heart remains relatively normal in pediatric subjects with OSAS. However, baseline cardiovascular sympathetic activity is elevated, and reactivity to autonomic challenges is impaired.

Keywords: pediatric sleep disordered breathing, autonomic nervous system, mathematical model, respiratory sinus arrhythmia, baroreflex

Citation: Chaicham J; Lin Z; Chen ML; Ward SLD; Keens T; Khoo MCK. Model-based assessment of cardiovascular autonomic control in children with obstructive sleep apnea. *SLEEP* 2009;32(7):927-938.

ALTHOUGH OBSTRUCTIVE SLEEP APNEA SYNDROME (OSAS) OCCURS QUITE FREQUENTLY IN THE PEDIATRIC POPULATION, WITH A PREVALENCE RATE OF 1 TO 3% in preschool-aged children,¹ the cardiovascular consequences of OSAS in children have been less extensively studied, compared with the adult form of sleep-disordered breathing. Most studies have suggested a causal link between OSAS and cardiovascular disease in adults,²⁻⁴ primarily in the form of systemic hypertension, myocardial infarction, and stroke. Cardiovascular disease has also been reported to occur in children with severe OSAS, but the more common manifestations are pulmonary hypertension; compromised right ventricular function, including cor pulmonale; and congestive heart failure.^{5,6} The cumulative evidence in adults suggests that autonomic dysfunction, in the form of reduced parasympathetic activity and elevated sympathetic tone, plays an important role in mediating the link between OSAS and cardiovascular disease.²⁻⁴ In contrast, the chronic effects of OSAS on autonomic function in children have been little studied.⁶ In this study, we hypothesize that the autonomic nervous system is also adversely affected in pediatric OSAS but that the relative impact on the parasympathetic and sympathetic branches differs from what occurs in adults.

In recent years, it has become increasingly popular to employ spectral analysis of heart rate variability (HRV) as a simple and cost-effective tool for noninvasive assessment of autonomic function.⁷ The power of the HRV spectrum in the frequency range of 0.15 to 0.4 Hz, referred to as *high-frequency power* (HFP), is frequently taken to quantify vagal tone. On the other hand, HRV power from 0.04 to 0.15 Hz, referred to as *low-frequency power* (LFP), has been shown to reflect both sympathetic and parasympathetic activity.⁸ The ratio (LHR) between LFP and HFP is therefore known as representing an index of *sympathovagal balance*,⁸ with a higher LHR implying a shift toward sympathetic dominance, a decrease in vagal tone, or both.⁹ The underpinnings of HRV spectral analysis are derived largely from the 1975 study of Katona and Jih,¹⁰ which demonstrated, in an animal preparation, a linear relationship between respiratory-related fluctuations in R-R intervals (RRI) and vagal firing rates. Studies using HRV for autonomic-function assessment often overlook the fact that this key observation and the other validation findings that followed¹¹ were obtained under conditions in which respiration was relatively well controlled. However, it has been shown that changes or differences in breathing frequency, tidal volume, or ventilatory pattern can significantly confound the interpretation of autonomic activity that one derives from HRV spectral analysis.^{12,13} Some interventions that increase sympathetic drive also lead to increases in LFP of blood-pressure variability (BPV).⁸ Thus, the power of low-frequency BPV oscillations has been proposed by some to represent a quantitative index of sympathetic modulation of the peripheral vasculature. At the same time, however, there are other observations that do not support this view.⁹

Submitted for publication September, 2008

Submitted in final revised form March, 2009

Accepted for publication April, 2009

Address correspondence to: Michael C.K. Khoo, PhD, Biomedical Engineering Department, University of Southern California, DRB-140, University Park, Los Angeles, CA 90089-1111; Tel: (213) 740-0347; E-mail: khoo@bmsr.usc.edu

Table 1—Participant Characteristics

Control subjects				Subjects with OSAS				
Participant	Age, y	BMI, kg/m ²	Sex	Participant	Age, y	BMI, kg/m ²	AHI	Sex
N1	12.3	22.7	M	O1	10.2	23.0	11	F
N2	9.9	16.8	M	O2	11.1	21.8	14	F
N3	8.2	17.7	F	O3	10.2	24.6	8.3	F
N4	10.2	18.4	F	O4	10.5	30.8	52	M
N5	15.6	22.3	M	O5	11.4	15.7	16	M
N6	16.7	20.2	F	O6	10.1	17.9	15	F
N7	11.5	17.8	M	O7	14.0	26.4	30	F
N8	8.3	16.8	M	O8	12.0	33.3	49	F
N9	11.5	15.5	F	O9	10.7	31.0	10	M
N10	11.4	14.9	M	O10	14.1	33.1	5	F
Mean	11.5	18.3		Mean	11.4	25.8	21.0	
SEM	3.7	5.8		SEM	3.6	8.1	6.6	

Note: BMI refers to body mass index; AHI, apnea-hypopnea index, the number of apneas and hypopneas per hour of sleep.

To circumvent the limitations associated with spectral analysis of HRV or BPV, we have developed an alternative approach for noninvasive assessment of autonomic function. This approach employs a closed-loop model that relates HRV to respiration and BPV and relates BPV to changes in heart rate and respiration. The model has been validated in a number of studies on adult subjects with OSAS and normal control subjects under a variety of conditions.¹⁴⁻¹⁷ For instance, our group has shown that continuous positive airway pressure therapy in subjects with OSAS leads to improved autonomic function, as reflected in cardiovascular variability.¹⁴ In another study, we showed that autonomic control is impaired in subjects with OSAS during both wakefulness and sleep.^{15,16} We recently extended the model so that temporal changes in the parameters can be estimated when data are collected under time-varying conditions, such as during arousals from sleep.^{17,18}

In this study, we applied both the original and time-varying versions of the closed-loop model to assess cardiovascular autonomic control in pediatric OSAS under conditions of altered orthostatic stress and cold face stimulation (CFS). Changing posture from supine to standing is known to increase sympathetic drive and decrease vagal tone. The CFS test activates the diving reflex, which produces an increase in systemic vascular resistance via an elevation of peripheral sympathetic activity, along with a concomitant bradycardia as a consequence of increased vagal drive.^{19,20} The combination of the 2 autonomic tests thus allowed us to determine how the model parameters would be affected by conditions in which vagal and sympathetic activity are altered in opposite directions (orthostatic stress), as well as in the same direction (CFS).

METHODS

Participants

Ten pediatric patients with moderate to severe OSAS (obstructive apnea-hypopnea index = 21 ± 5.3 /h) before treatment and 10 normal control subjects were recruited. The normal control subjects were selected only if the subject's parents affirmed that their child did not snore at all; subjects who snored oc-

asionally were excluded and so were those who had a cold or upper respiratory infection. Subjects in the OSAS group were selected if their apnea-hypopnea index (AHI) was greater than or equal to 5, based on the outcome of a prior polysomnographic study. Subjects with OSAS that was believed to be related to craniofacial abnormality or genetic syndromes were excluded. None of the subjects had a history of lung disease, cardiac arrhythmia, congestive heart failure, or diabetes. They all were screened with a pulmonary function test for abnormal lung mechanics; the result was negative in all subjects. The study was approved by the Committee on Clinical Investigations (institutional review board) of Childrens Hospital Los Angeles. Written informed consent was obtained from the parents of each subject before participation in the study. Assent was obtained from the subjects themselves.

The average age of the OSAS group was 11.4 ± 0.5 years, and the subjects had a mean BMI of 25.7 ± 2 kg/m²; the average age of the control group was 11.5 ± 0.9 years, and the subjects had a mean BMI of 18.3 ± 0.8 kg/m² (Table 1). Thus, average BMI was larger in the OSAS group versus the control group ($P = 0.007$). All of the subjects with OSAS had overt tonsillar hypertrophy. Table 2 summarizes the results of the polysomnographic studies performed on the subjects with OSAS prior to the start of this research study.

Experimental Procedures and Data Preprocessing

The experimental protocol consisted of 3 parts: (1) spontaneous breathing in the supine posture for 15 to 20 minutes (baseline condition); (2) spontaneous breathing during standing for 15 to 20 minutes (orthostatic stress); and (3) (CFS, after the participant rested for 3 minutes in supine wakefulness, a gel pack (cooled to 0°C) was placed on the participant's forehead for 1 minute and was subsequently removed while recording continued for another 5 minutes. During the experiments, noninvasive continuous blood pressure (using a Model 7000 arterial wrist tonometer, Colin Medical Instruments, San Antonio, TX), electrocardiogram (by 3-lead electrocardiogram, BMA-831 bio-amplifier, CWE, Ardmore, PA), and respiratory air flow (by pneumotachometer, model 3700, Hans Rudolph, Kansas

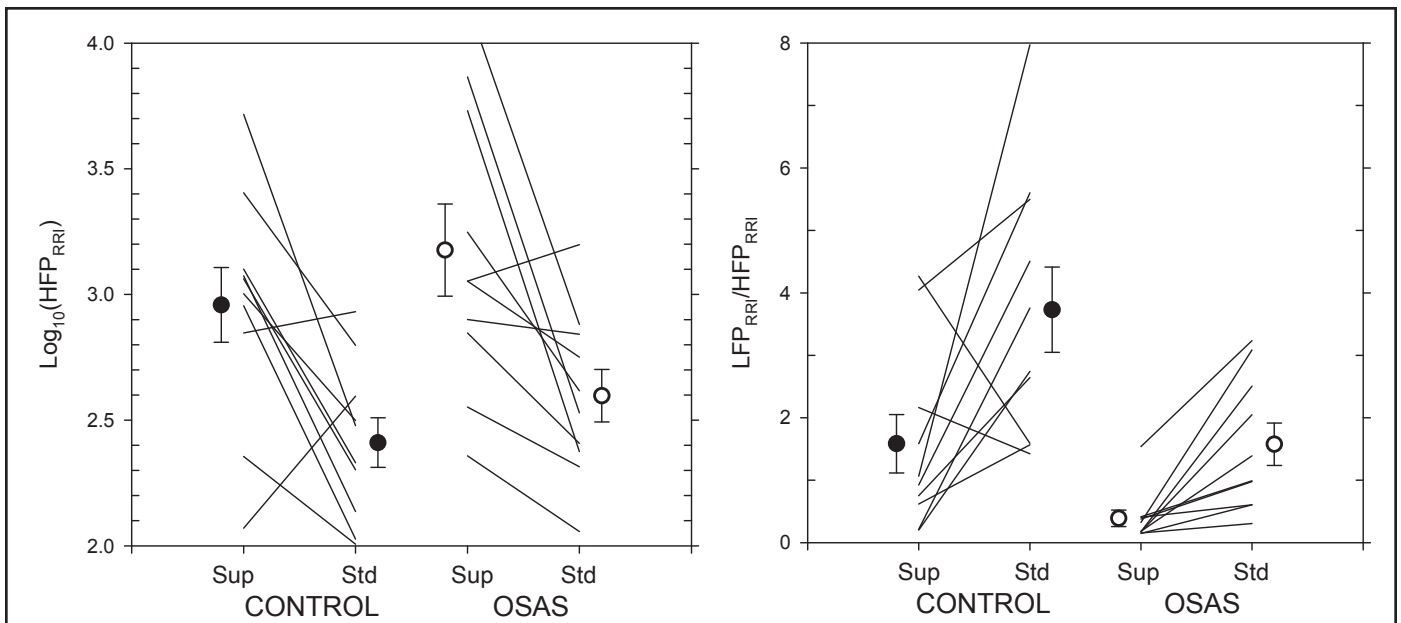


Figure 2—Effects of orthostatic stress on the spectral indices of heart rate variability (HFP_{RRI} and LHR) in control subjects (CONTROL) and subjects with obstructive sleep apnea syndrome (OSAS). Lines depict how HFP_{RRI} (left panel) and LHR (right panel) change in individual subjects. The circles and error bars represent group means and SEM. See Appendix 2 for definition of abbreviations.

sibility that the mechanical effect of respiration on blood pressure could be virtually instantaneous; hence, no delay was assumed in this case. $_{RRI}(t)$ and $_{SBP}(t)$ represent the discrepancy (error) between the model predictions and the corresponding RRI and SBP measurements, respectively, reflecting those aspects of the data that are not explained by the model.

The Meixner expansion of kernels technique²³ was used to estimate the unknown impulse responses h_{RCC} , h_{ABR} , h_{CID} , and h_{DER} . The least-squares minimization procedure was repeated for a range of values for the delays ($_{ABR}$ and $_{RCC}$), the order of generalization (n from 0 to 5), and Meixner function orders (q_{ABR} and q_{RCC} from 4 to 8). For each combination of delays, the order of generalization and Meixner function orders—a metric of the quality of f_t , known as the “minimum description length” (*MDL*)—was computed.²⁴ Selection of the *optimal* candidate model was based on a global search for the minimum *MDL*; in addition, this *optimal* solution had to satisfy the condition that the cross-correlations between the residual errors and past values of the 2 inputs ($V(t)$ and $SBP(t)$) were statistically indistinguishable from 0. Details of the time-varying version of this model are given in Appendix 1.

The estimation of the above impulse responses was improved by increasing the orthogonality between the 2 inputs. This was achieved by using an autoregressive model with exogenous input (ARX model) to filter out the RCC from SBP . Respiration and the respiration-uncorrelated SBP were used as dual inputs to the model, as represented in Equation (2). Subsequently, the calculated $h_{ABR}(t)$ was kept unchanged while estimation of $h_{RCC}(t)$ was repeated using the respiration and original (un-orthogonalized) blood pressure inputs. This technique was also applied to estimate $h_{CID}(t)$ and $h_{DER}(t)$.

Once each model-component impulse response was estimated, the corresponding transfer function was computed by applying the fast Fourier transform for conversion to the frequency

domain. Subsequently, the following descriptors were extracted from each transfer function: (1) the overall dynamic gain (DG) or the average transfer function magnitude between 0.04 and 0.4 Hz; (2) the high-frequency gain (HFG), the average transfer function magnitude between 0.15 and 0.4 Hz; and (3) the low-frequency gain (LFG), the average transfer function magnitude between 0.04 and 0.15 Hz.

Other Calculations

For each dataset, the following descriptors were also calculated: (1) the mean values of RRI and SBP for the data segment in question, (2) the spectral indices of HRV: HFP_{RRI} and LHR, (3) and the FLP (LFP_{SBP}) of the SBP time course. The spectral indices were computed using the Blackman-Tukey method of spectral analysis.¹⁵

Statistical Tests

For the orthostatic stress results, 2-way repeated measures analysis of variance (ANOVA) was applied to each of the estimated model descriptors. The first (unrepeated) factor was Participant Group (control vs OSAS), whereas the other (repeated) factor was Condition (supine vs standing). If the 2-way repeated measures ANOVA indicated significant differences in the factors or their interaction, posthoc pairwise comparisons were performed using the Holm-Sidak method. In CFS, the percentage change of each feature from pre-CFS (an average of 1 minute of feature before the test) was calculated. Subsequently, 2 minutes of the percentage change of each feature were averaged every 5 seconds. Subsequently, 2-way repeated measures ANOVA was performed in which 1 factor (unrepeated) was Participant Group (control vs OSAS) and the other (repeated) factor was Time from Start of CFS. These analyses were re-

Table 3— Summary Cardiovascular Measures and Spectral Indices of Heart Rate and Blood Pressure Variability

Cardiovascular Measure	Supine ^a		Standing ^a		Group	P Values	
	Control	OSAS	Control	OSAS		Condition	Group x Condition
Mean RRI, ms	785 ± 34.7	803.6 ± 36.6 ^b	580.6 ± 47.7 ^c	601.2 ± 31.2 ^c	0.103	< 0.001	0.079
Mean blood pressure, mm Hg							
Systolic	104.9 ± 4.4	98.2 ± 5.7	96.2 ± 9.25	83.4 ± 7.93	0.742	0.446	0.110
Diastolic	52.2 ± 3.4	41.3 ± 5.2	58.2 ± 2.7	44.8 ± 6.4	0.033	0.249	0.768
HFP _{RRI} , ms ²	1430 ± 469	3321 ± 1438	325.3 ± 77.4	516 ± 136 ^c	0.192	0.018	0.274
LHR	1.6 ± 0.5	0.39 ± 0.13	3.73 ± 0.68 ^c	1.58 ± 0.34 ^b	0.002	0.002	0.296
LFP _{SBP} (mmHg ²)	4.8 ± 2.1	8.2 ± 2.6	17.88 ± 6.33	32.37 ± 8.16 ^c	0.168	< 0.001	0.232

^aData are presented as mean ± SEM. OSAS refers to obstructive sleep apnea syndrome; see Appendix 2 for definition of abbreviations.

^bSignificantly different from controls in the same condition. ^cSignificantly different from the same group in supine condition.

peated using only a subset of participants (Table 1, N1 to N7 and O1 to O7—ie, the control subjects with the lowest BMI and the OSAS subjects with the highest BMI were rejected), who were roughly matched for BMI (19.41 ± 2.35 vs 22.89 ± 5.07). All statistical procedures were implemented using SigmaStat for Windows software (SPSS; Chicago, IL).

RESULTS

Cardiovascular Responses

Orthostatic Stress

Table 3 summarizes the effects of postural change from supine to standing on the mean values of RRI and blood pressure, as well as the spectral indices of HRV and BPV. Mean RRI was higher (or, equivalently, mean heart rate was lower) in subjects with OSAS versus control subjects in both supine and standing; however, in both groups, mean RRI decreased from supine to standing. Mean SBP was not different between groups and did not change with posture. However, mean DBP was lower in subjects with OSAS relative to the control subjects. The power of the high-frequency component of HRV (HFP_{RRI}) displayed a tendency to be higher in subjects with OSAS, but this difference was not statistically significant. On the other hand, LHR was lower in subjects with OSAS ($P = 0.002$). Low-frequency blood pressure variability, represented by LFP_{SBP}, tended to be higher in the subjects with OSAS, but this did not attain statistical significance.

Figure 2 shows the values of HFP_{RRI} and LHR in the individual subjects, along with how each of these values changed with orthostatic stress. In both subject groups, standing led to a significant drop in HFP_{RRI} and an increase in LHR. It is clear from Figure 2 that there was also substantial variability in HFP_{RRI} and LHR across subjects within each group.

Cold Face Stimulation

Figure 3 illustrates the group-averaged time courses for RRI (top panel), SBP (middle panel), and ventilation (bottom panel) exhibited by the control and OSAS subjects during application of CFS. The time courses have been displayed in terms of percentage changes from each subject's baseline 1

minute prior to application of the cold stimulus. Both subject groups responded to CFS with a small but significant degree of bradycardia, accompanied by a rise in SBP. Whereas the control subjects showed a steady and substantial rise in SBP, the time course of SBP in the subjects with OSAS was more variable and displayed a dip back toward baseline in the middle of the CFS procedure. The total increase in SBP in the subjects with OSAS at the end of the CFS was approximately half as large as that in the control subjects. In both groups, the ventilation time courses also displayed significant fluctuations during CFS, thus underscoring the need to take into account respiratory variability when using HRV or BPV for autonomic assessment purposes.

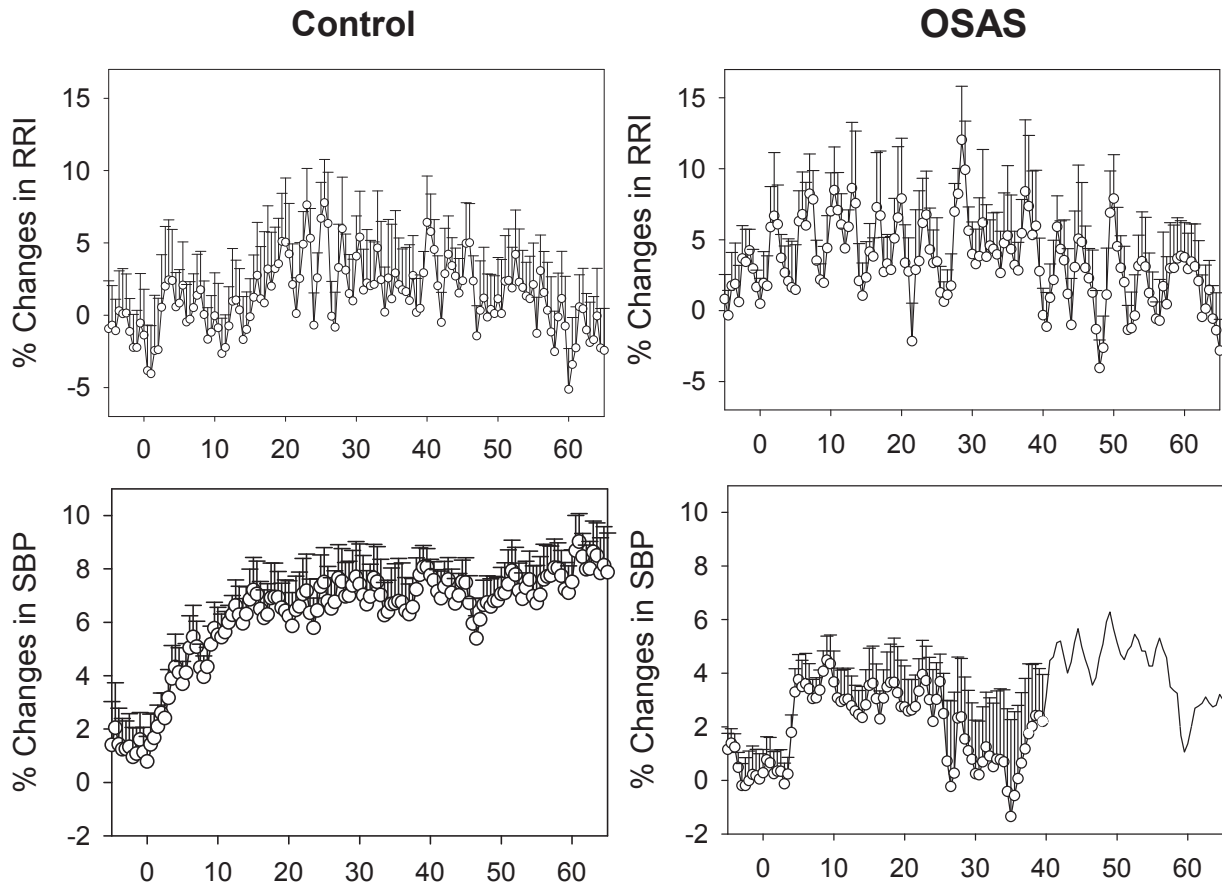
Changes in Minimal Model Parameters

Orthostatic Stress

The average values of the descriptors derived from the estimated-model component-transfer functions are displayed in Table 4. There were no differences in RCC gains between the subject groups; in both groups, standing led to significant reductions in all RCC gains. Baroreflex low-frequency gain (LFG_{ABR}) and overall dynamic gain (DG_{ABR}) were lower in subjects with OSAS relative to control subjects in both postures. As well, all parameters related to baroreflex gain decreased with change of posture from supine to standing, but the reductions were smaller in subjects with OSAS. There was no significant difference between the DER gains estimated in subjects with OSAS versus normal control subjects. However, both groups showed strong increases in all DER gains when postural change was imposed. Similarly, the CID gains were not different between subject groups. However, in the control group, CID gain increased substantially with standing, while there was little or no change in the corresponding gains in the subjects with OSAS.

Cold Face Stimulation

The group-averaged estimates of the time courses during CFS for the model parameters, computed using the time-varying algorithm, are displayed in Figure 4. As in Figure 3, the magnitude of changes in these time courses represent percentage changes from the average of the 1-minute period imme-



diately prior to application of the cold stimulus. ABR gain increased steadily during the CFS in both subject groups, displaying no difference in time course. RCC gain also increased in both groups during CFS and remained similar until after 30 seconds following the start of CFS, when this parameter increased more rapidly in the control subjects. In contrast, CID gain trended higher during CFS in the control subjects but remained relatively unchanged in subjects with OSAS. DER gain also increased progressively in control subjects during CFS but became only slightly elevated above baseline in subjects with OSAS.

DISCUSSION

Comparison with Other Studies of Autonomic Function in Pediatric OSAS

In contrast with the extensive literature that is available on adult humans, few studies have investigated the effects of OSAS on the autonomic nervous system activity in children. In particular, none have examined autonomic function in OSAS children in daytime wakefulness. Two studies^{25,26} reported elevated blood pressure during overnight polysomnography, but

Table 4—Comparison of Estimated Model Parameters and Spectral Indices for All Participants (Control vs OSAS in the Supine & Standing Positions)

Model Descriptors	Supine ^a		Standing ^a		P Values		
	Control	OSAS	Control	OSAS	Group	Condition	Group x Condition
RCC							
LF	1.07 ± 0.2	1.2 ± 0.3	0.62 ± 0.16	0.64 ± 0.11 ^c	0.739	0.012	0.769
HF	1.48 ± 0.2	1.6 ± 0.4	0.63 ± 0.16 ^c	0.74 ± 0.18 ^c	0.631	0.003	0.970
OA	1.35 ± 0.2	1.5 ± 0.3	0.62 ± 0.15 ^c	0.71 ± 0.15 ^c	0.644	0.002	0.917
ABR							
LF	0.033 ± 0.006	0.014 ± 0.002 ^b	0.023 ± 0.004 ^c	0.009 ± 0.002 ^b	0.002	0.029	0.431
HF	0.028 ± 0.008	0.017 ± 0.006	0.012 ± 0.003	0.006 ± 0.003	0.128	0.032	0.649
OA	0.029 ± 0.007	0.016 ± 0.004	0.015 ± 0.003 ^c	0.007 ± 0.003	0.031	0.026	0.590
DER							
LF	0.039 ± 0.008	0.053 ± 0.011	0.10 ± 0.016 ^c	0.10 ± 0.017 ^c	0.702	< 0.001	0.537
HF	0.032 ± 0.007	0.036 ± 0.009	0.094 ± 0.013 ^c	0.12 ± 0.025 ^c	0.389	< 0.001	0.402
OA	0.034 ± 0.007	0.041 ± 0.009	0.097 ± 0.012 ^c	0.12 ± 0.021 ^c	0.430	< 0.001	0.590
CID							
LF	2.08 ± 0.3	3.2 ± 0.3	3.19 ± 0.73	2.69 ± 0.35	0.537	0.479	0.044
HF	1.4 ± 0.2	2.0 ± 0.3	2.80 ± 0.45 ^c	2.24 ± 0.17	0.999	0.005	0.034
OA	1.6 ± 0.2	2.4 ± 0.3	2.92 ± 0.53 ^c	2.38 ± 0.17	0.792	0.027	0.026

^aData are shown as mean ± SEM. OSAS refers to obstructive sleep apnea syndrome; see Appendix 2 for definition of abbreviations. ^bSignificantly different from control subjects in the same condition. ^cSignificantly different from the same group in supine condition.

another²⁷ found no difference in SBP between subjects with OSAS and primary snorers, although DBP was significantly higher in subjects with OSAS. Amin et al.²⁸ found no difference in SBP or mean arterial pressure among primary snorers or those with mild OSAS and moderate to severe OSAS, but they did find a significantly lower DBP in subjects with moderate to severe OSAS. These apparent contradictions across studies have arisen in part because of the small differences in blood pressure between subjects with OSAS and control subjects, underscoring the need for more sensitive (noninvasive) indicators of autonomic function.

Aljadeff et al.²⁹ compared HRV during overnight sleep between pediatric subjects with OSAS and normal control subjects, but the study focused on the acute effects of episodic apnea or hypopnea on the beat-to-beat patterning of heart rate. Baharav et al.³⁰ employed HRV spectral analysis to assess autonomic cardiac control in children with OSAS and normal control subjects in overnight sleep studies. They found normalized HFP_{RRI} to be lower in the subjects with OSAS during rapid eye movement sleep and during wakefulness just prior to sleep onset. LHR in the subjects with OSAS was found to be higher relative to control subjects during the period of wakefulness immediately before the onset of sleep, slow-wave sleep, and rapid eye movement sleep. In contrast, our study, conducted only in daytime wakefulness, showed, in subjects with OSAS, that baseline (supine) LHR was lower versus that of control subjects, whereas HFP_{RRI} was not significantly different. These results fall in contradistinction to what has been reported in adults with OSAS^{14,15} during wakefulness, not to mention Baharav's study, although the latter was carried out during sleep. On the other hand, our findings of a reduction in HFP_{RRI} and increase in LHR with orthostatic stress within subjects in both groups are consistent with the well-known decrease in vagal drive and increase in sympathetic tone that accompany postural changes from supine to upright.^{8,9} The increase in low-

frequency blood-pressure oscillations, LFP_{SBP} that appeared in both subject groups as a consequence of orthostatic stress is also consistent with the shift toward sympathetic predominance that accompanies standing. There are some possible explanations for our unexpected finding of a lower LHR and no significant differences in HFP_{RRI} in the OSAS group versus control subjects. The first and most straightforward interpretation is that the subjects with OSAS have normal levels of vagal activity but decreased sympathetic activity. This possibility seems quite unlikely and would be totally inconsistent with what has been learned about the chronic effects of intermittent hypoxia on the sympathetic nervous system. As well, decreased sympathetic modulation does not always imply reduced sympathetic tone. Indeed, it has been shown that low-frequency modulation of heart rate (and thus, LHR) can become virtually undetectable in patients with severe heart failure³¹ or under conditions of severe exercise in normal subjects,³² even though sympathetic drive is known to be elevated. Indeed, employing HRV alone to assess autonomic tone has been likened to using the height of waves to predict the depth of the ocean at a given location.³³ A second potential explanation for our finding is that the ventilatory patterns of some of the subjects during the short (< 20-min duration) periods of measurement may have been affected by the highly controlled conditions of the experiments, and these may have confounded the HRV spectral indices of the subjects. For instance, we have shown that LHR can be altered dramatically in a given subject depending on the subject's breathing rate and pattern.³⁴ The third possibility, which we consider to be the most likely explanation, is given below.

Changes in Minimal Model Parameters

The preceding section underscores some of the potential pitfalls of relying solely on HRV spectral indices to draw conclusions regarding autonomic function. These issues are not

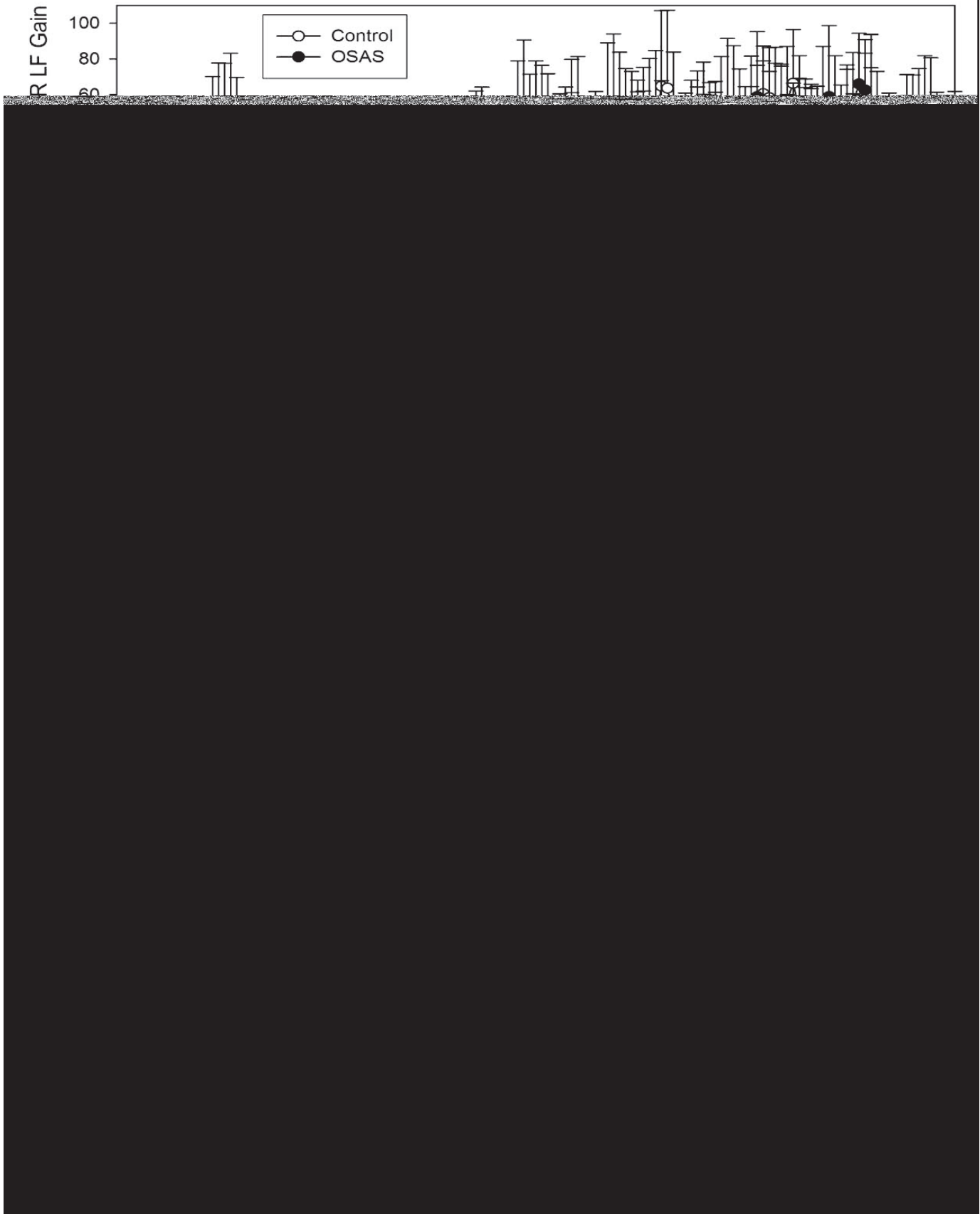


Figure 4—Percentage change in ABR, RCC, CID, and DER gains during cold face stimulation (CFS). Circles and error bars represent group mean \pm SEM. CFS started at time 0. See Appendix 2 for definition of abbreviations.

unique to the present study but have been raised in other studies involving adult subjects.³⁵ A key problem with spectral analysis of HRV or BPV is that it only yields information about the output (ie, fluctuations in heart rate or blood pressure) of the underlying system and provides little insight into the reflex mechanisms that may have contributed to the output. To circumvent this limitation, we analyzed our measurements using a closed-loop minimal model of autonomic cardiovascular control. The model enabled the characterization of the dynamic interrelationships between various pairings of the key variables (respiration, RRI, SBP) in play, hence providing invaluable information about the underlying system that could not otherwise have been obtained through univariate analyses of HRV or BPV. The model-based approach also allowed us to dissociate the confounding effects of respiration from other sources that contribute to HRV and BPV.

Under baseline conditions, we found that baroreflex (ABR) gain was approximately half as large in subjects with OSAS versus control subjects but that there were no differences in the other minimal model parameters (Table 3). The RCC component of the model represents the transfer function between respiration and HRV. The similarity of RCC gain between the control subjects and those with OSAS is therefore compatible with our finding of the lack of any difference in baseline HFP_{RRI} between the 2 subject groups. This may be due to the fact that there is a large reserve of parasympathetic tone in children that decrease with aging.³⁶

Since the baroreflexes are known to be responsible for mediating a significant fraction of the low-frequency oscillations in HRV,^{8,9} the substantially reduced ABR gain that we have found in the subjects with OSAS is consistent with our earlier finding of decreased LFP_{RRI} (and, thus, LHR) in these subjects. Blunted baroreflex sensitivity is found in patients with heart failure³⁷ and in normal subjects during severe exercise,³² coincident with substantial reductions in LFP_{RRI} . Impaired baroreflex sensitivity is also known to be associated with elevated sympathetic drive.³⁷ Thus, the reduced ABR gain found in our subjects with OSAS is compatible with a high sympathetic tone in these individuals.

Orthostatic stress led to a significant reduction in RCC gain in both groups, reflecting a decrease in vagal tone due to postural change. ABR gain also decreased with orthostatic stress, but the change was not as pronounced in the OSAS group, since this gain was already low in the supine condition. DER gain increased from supine to standing in both subject groups, whereas CID gain increased with orthostatic stress in only the control subjects. These findings are consistent with a reduced sympathetic reactivity to postural change, along with an elevated baseline level of sympathetic tone in subjects with OSAS.

Adjustment for Potential BMI Effects

We considered the possibility that the larger average BMI of the subjects with OSAS may exert a confounding influence on the results displayed in Table 3. To counter this potential problem, we eliminated 3 subjects with OSAS who had the largest BMI, as well as 3 control subjects with the lowest BMI. This reduction of the outliers in each group helped to make the remaining groups roughly matched in BMI. Values of the estimat-

ed model parameters for the subsets of the 2 groups, following adjustment for BMI, are shown in Table 4. As in the larger sample set, RCC gains were not different between the groups but decreased in both groups with postural change from supine to standing. ABR gain remained significantly lower in subjects with OSAS versus control subjects. DER gains increased with standing in both groups. As was found in the larger sample, CID gains increased with standing only in the control subjects but not in the subjects with OSAS. These findings suggest that the differences predicted by our model are relatively robust and not likely to be a consequence of the confounding influence of obesity.

Cold Face Stimulation

Cold face stimulation led to a similar degree of transient bradycardia in both subjects with OSAS and control subjects, but the responses were much more variable in those with OSAS. Although CFS produced a robust increase in SBP in the control subjects, the corresponding blood pressure response in the subjects with OSAS was weaker and more variable. The ventilatory responses also appeared to be different between subject groups but varied considerably across subjects within each group.

By analyzing these responses within the framework of the time-varying minimal model, we found that RCC and ABR gains increased with CFS along time courses that were similar between the subjects with OSAS and control subjects. In the model, BPV (Δ SBP) is assumed to be related to respiration through the DER component, as well as to the fluctuations in the ratio between pulse pressure and heart period (Δ SCO, see Figure 2). Thus, total peripheral resistance and arterial compliance are implicitly factored into the CID impulse response. We found the assumption of time invariance for the CID kernel to be a limiting factor, allowing the minimal model to account for less than 60% of the total variance in Δ SBP. We reasoned that, since total peripheral resistance is modulated by sympathetic drive, which is time varying, allowing the CID gain to be time varying would be 1 way of allowing the model to incorporate this feature. By allowing the CID gain to vary with time, we were able to substantially reduce the variance of the discrepancies between the measured blood pressure measurements and the model predictions to less than 25%. Low-frequency fluctuations were apparent in the estimated time-varying CID gains (Figure 4), consistent with observations of low-frequency fluctuations in sympathetic modulation of the peripheral vasculature. Autonomic reactivity, as represented by the changes in CID gain in response to CFS, is different between the groups. In control subjects, CID gain increased with CFS, whereas, in OSAS, CID gain remained unchanged or decreased slightly.

Our model-based analyses of the CFS responses suggest that, although vagal reactivity remains relatively intact in pediatric subjects with OSAS, cardiovascular sympathetic reactivity is impaired. O'Brien and Gozal³⁶ concluded that the sympathetic branch of the autonomic nervous system is abnormal in OSAS, but their results suggest that cardiovascular sympathetic reactivity is overexpressed in OSAS, whereas our findings suggest a blunting of sympathetic reactivity. A potential explanation for this discrepancy is that the autonomic challenges that were employed in our studies and O'Brien's

were quite different: the latter group used a vital capacity sigh or the cold pressor test to elicit peripheral vasoconstriction, whereas, in our study, we used the CFS test, which elicits an increase in vagal activity along with an increase in sympathetic activity. However, our results on the effects of orthostatic stress on CID gain are consistent with our findings on the effects of CFS, in that both indicate a blunted sympathetic reactivity in the OSAS subjects.

Limitations of the Study

There are a number of limitations in this study. First, the subjects in our control group were not studied by polysomnography, and, thus, it is not possible to definitively rule out occult mild OSA in some individuals. However, we believe that the presence of OSA in the control subjects is unlikely, since they were selected only if the subject's parents affirmed that their child did not snore at all; we screened out subjects who snored occasionally, as well as nonsnorers who had a cold or upper respiratory infection. In a study involving more than 900 children aged 8 to 11 years, Rosen et al³⁹ found that snorers were 6.4 times more likely to have obstructive apnea of at least mild severity (AHI = 1) as compared with nonsnorers. Moreover, if we were to assume that some of the control subjects did have mild OSAS, the fact that we found significant differences in autonomic control between the 2 groups implies that these differences would have remained in the same direction and would have been even larger had the subjects with hypothetical mild OSAS been properly screened out of the control group.

A second potential limitation is that subjects with different etiologies of OSAS may exhibit different levels of autonomic abnormalities. To minimize this possibility, we excluded from our subject pool individuals who had OSAS related to craniofacial abnormality or a genetic syndrome. By including only those subjects with OSAS who had overt tonsillar hypertrophy and were otherwise healthy, a subset of whom were overweight, we believe we limited the potential etiologies to the 2 most common ones in childhood, which is representative of the clinical population.

Conclusion

In summary, we employed spectral analysis of HRV and BPV along with model-based analysis to compare baseline autonomic function and autonomic reactivity in subjects with OSAS with the corresponding results in normal control subjects. The model-based analysis produced results that are compatible with the findings deduced from spectral analysis, and the former has proven to be useful in enabling us to better interpret our measurements of HRV and BPV. Our present findings suggest that parasympathetic activity remains relatively normal in pediatric OSAS, but both baseline cardiovascular sympathetic activity and reactivity to autonomic challenges are impaired.

ACKNOWLEDGMENTS

This work was supported by NIH Grants EB-001978, HL076375, and HL-090451.

DISCLOSURE STATEMENT

This was not an industry supported study. The authors have indicated no financial conflicts of interest.

REFERENCES

1. American Thoracic Society. Cardiorespiratory sleep studies in children: establishment of normative data and polysomnographic predictors of morbidity. *Am J Respir Crit Care Med* 1999;160:1381-1387.
2. Somers VK, Dyken ME, Clary MP, Abboud FM. Sympathetic neural mechanisms in obstructive sleep apnea. *J Clin Invest* 1995;96:1897-904.
3. Leung RST, Bradley TD. Sleep apnea and cardiovascular Disease. *Am J Respir Crit Care Med* 2001;164:2147-65.
4. Caples SM, Gami AS, Somers VK. Obstructive sleep apnea. *Ann Intern Med* 2005;142:187-97.
5. Carroll JL, Loughlin GM. Obstructive sleep apnea syndrome in infants and children: clinical features and pathophysiology. In: Ferber R, Kryger M, eds. *Principles and Practice of Sleep Medicine*. Philadelphia, PA: Saunders; 1995:163-191.
6. Marcus CL. Sleep-disordered breathing in children. *Am J Respir Crit Care Med* 2001;164:16-30.
7. Task Force of the European Society of Cardiology and the North American Society of Pacing and Electrophysiology. Heart rate variability: standards of measurement, physiological interpretation and clinical use. *Circulation* 1996;93:1043-65.
8. Malliani A, Pagani M, Federico L, Cerutti S. Cardiovascular neural regulation explored in the frequency domain. *Circulation* 1991;84:482-92.
9. Malpas SC. Neural influences on cardiovascular variability: possibilities and pitfalls. *Am J Physiol* 2002;282:H6-20.
10. Katona PG, Jih F. Respiratory sinus arrhythmia: noninvasive measure of parasympathetic cardiac control. *J Appl Physiol* 1975;39:801-6.
11. Berntson GG, Bigger JT, Jr, Eckberg DL, et al. Heart rate variability: origins, methods, and interpretive caveats. *Psychophysiology* 1997;34:623-48.
12. Brown TE, Beightol LA, Koh J, Eckberg DL. Important influence of respiration on human RR interval power spectra is largely ignored. *J Appl Physiol* 1993;75:2310-17.
13. Khoo M C, Kim T S, Berry R B. Spectral indices of cardiac autonomic function in obstructive sleep apnea. *Sleep* 1999;22:443-51.
14. Belozeroff V, Berry RB, Sassoan CSH and Khoo MCK. Effects of CPAP therapy on cardiovascular variability in obstructive sleep apnea: a closed loop analysis. *Am J Physiol Heart Circ Physiol* 2002;282:H110-21.
15. Belozeroff V, Berry RB, Khoo MCK. Model-based assessment of autonomic control in obstructive sleep apnea syndrome. *Sleep* 2003;1:65-73.
16. Jo JA, Blasi A, Valladares E, Juarez R, Baydur A and Khoo MCK. A nonlinear model of cardiac autonomic control in obstructive sleep apnea syndrome. *Ann Biomed Eng* 2007;35:1425-43.
17. Blasi A, Jo JA, Valladares E, Juarez R, Baydur A and Khoo MCK. Autonomic cardiovascular control following transient arousal from sleep: A time-varying closed-loop model. *IEEE Trans Biomed Eng* 2006;53:74-82.
18. Chaicharn J, Carrington M, Trinder J and Khoo MCK. The effects on cardiovascular autonomic control of repetitive arousal from sleep. *Sleep* 2008;31:93-103.
19. Finley JP, Bonet JF, Waxman MB. Autonomic pathways responsible for bradycardia on facial immersion. *J Appl Physiol* 1979;47:1218-22.

20. Heistad DD, Abboud FM, Eckatein JW. Vasoconstrictor response to simulated diving in man. *J Appl Physiol* 1968;25:542-9.
21. Berger RD, Akselrod S, Gordon D, Cohen RJ. An efficient algorithm for spectrum analysis of heart rate variability. *IEEE Trans Biomed Eng* 1986;33:900-4.
22. Yang CCH, Kuo TBJ. Assessment of cardiac sympathetic regulation by respiratory-related arterial pressure variability in the rat. *J Physiol (Lond)* 1999;515.3:887-96.
23. Asyali MH, Juusola M. Use of Meixner functions in estimation of Volterra Kernels of nonlinear systems with delay. *IEEE Trans Biomed Eng* 2005;52:229-37.
24. Rissanen J. Estimation of structure by minimum description length. *Circ Sys Sig Proc* 1982;1:395-406.
25. Enright PL, Goodwin JL, Sherrill DL, Quan JR, Quan SF. Blood pressure elevation associated with sleep-related breathing disorder in a community sample of white and Hispanic children: the Tucson Children's Assessment of Sleep Apnea Study. *Arch Pediatr Adolesc Med* 2003;157:901-4.
26. Kohyama J, Ohinata JS, Hasegawa T. Blood pressure in sleep disordered breathing. *Arch Dis Child* 2003;88:139142.
27. Marcus CL, Greene MG, Carroll JL. Blood pressure in children with obstructive sleep apnea. *Am J Respir Crit Care Med* 1998;157:1098-103.
28. Amin RS, Carroll JL, Jeffries JL, et al. Twenty-four-hour ambulatory blood pressure in children with sleep-disordered breathing. *Am J Respir Crit Care Med* 2004;169:950-6.
29. Aljadeff G, Gozal D, Schechtman VL, et al. Heart rate variability in children with obstructive sleep apnea. *Sleep* 1997;20:151-7.
30. Baharav A, Kotagal S, Rubin BK, Pratt J, Akselrod S. Autonomic cardiovascular control in children with obstructive sleep apnea. *Clin Auton Res* 1999;9:345-51.
31. van de Borne P, Montana N, Pagani M, Oren R, Somers VK. Absence of low-frequency variability of sympathetic nerve activity in severe heart failure. *Circulation* 1997;95:1449-54.
32. Casadei B, Cochrane S, Johnston J, Conway J, Sleight P. Pitfalls in the interpretation of spectral analysis of the heart rate variability during exercise in humans. *Acta Physiol Scand* 1995;153:125-31.
33. Malik M, Camm AJ. Components of heart rate variability—what they really mean and what we really measure. *Am J Cardiol* 1993;72:821-2.
34. Khoo MCK, Belozeroff V, Berry RB, Sassoos CSH. Cardiac autonomic control in obstructive sleep apnea: effects of long-term CPAP therapy. *Am J Respir Crit Care Med* 2001;164:807-12.
35. Sleight P, La Rovere MT, Mortara A, et al. Physiology and pathophysiology of heart rate and blood pressure variability in humans: is power spectral analysis largely an index of baroreflex gain? *Clin Sci* 1995;88:103-9.
36. Ingall TJ, McLeod JG, O'Brien PC. The effect of ageing on autonomic nervous system function. *Aust N Z J Med* 1990;20:570-7.
37. Francis DP, Coats AJS, Ponikowski P. Chemoreflex-baroreflex interactions in cardiovascular disease. In: Bradley TD, Floras JS, eds. *Sleep Apnea: Implications in Cardiovascular and Cerebrovascular Disease*. New York, NY: Marcel Dekker; 2000:33-60.
38. O'Brien LM, Gozal D. Autonomic dysfunction in children with sleep-disordered breathing. *Sleep* 2005;28:747-52.
39. Rosen CL, Larkin EK, Kirchner HL, et al. Prevalence and risk factors for sleep-disordered breathing in 8- to 11-year old children: association with race and prematurity. *J Pediatr* 2003;142:383-9.

APPENDIX 1

Estimation of the Model Impulse Responses

The stationary version of the model was used to analyze the data collected from the supine and standing conditions. To capture the dynamics of the changes occurring during the cold face stress test, this model was modified to allow the model parameter to be time varying.

To reduce the number of parameters to be estimated, each of the unknown impulse responses in Equation (2) was expanded as the sum of several weighted Meixner basis functions (MBF):²³

$$h_{ABR}(t) = \sum_{j=0}^{q_{ABR}-1} c_j^{ABR} B_j^{(n)}(t) \quad (A1)$$

$$h_{RCC}(t) = \sum_{j=0}^{q_{RSA}-1} c_j^{RCC} B_j^{(n)}(t) \quad (A2)$$

where the $B_j^{(n)}(t)$ represents the j -th order discrete-time orthonormal Meixner function with n -th order of generalization, which determines how late the MBF will start to fluctuate, and c_j^{ABR} and c_j^{RCC} are the corresponding unknown weights that are assigned to $B_j^{(n)}(t)$ in the ABR and RCC impulse responses, respectively. MBF are a generalization of the discrete Laguerre basis functions (LBF). First, the LBF were generated. Then, the LBF were transformed to MBF.²³ The j -th order LBF is defined as follows over the interval $0 \leq t \leq M-1$:

$$L_0(t) = \sqrt{\alpha^t(1-\alpha)} \quad (A3a)$$

and

$$L_j(t) = \sqrt{\alpha} L_j(t-1) + \sqrt{1-\alpha} L_{j-1}(t-1), \quad 0 \leq j \leq q_{ABR}, q_{RSA} \quad (A3b)$$

q_{ABR} and q_{RSA} represent the total number of Laguerre functions used in the expansion of the ABR and RCC impulse responses, respectively. In Equations (A3a) and (A3b), the parameter α ($0 < \alpha < 1$) determines the rate of exponential decline of the Laguerre functions, and is selected such that, for given M , q_{ABR} and q_{RSA} , the values of the constructed impulse response become insignificant as t approaches M . The orthogonal matrix that transforms the LBF to the MBF can be expressed as

$$A^{(n)} = X^{(n)} Y^{(n)} \quad (A4)$$

where $n=0,1,2,\dots$, and Y is an upper band matrix given as follows:

$$Y = \begin{bmatrix} 1 & \alpha & 0 & \dots & 0 \\ 0 & 1 & \alpha & \dots & 0 \\ 0 & 0 & 1 & \dots & 0 \\ \vdots & \vdots & \vdots & \ddots & \vdots \\ 0 & 0 & 0 & \dots & 1 \end{bmatrix}_{Q \times Q} \quad (A5)$$

and $X^{(n)}$ is an inversion of the Cholesky factorization of $Y^{(n)} \{Y^{(n)}\}^T$.

Substituting Equations (A1) and (A2) into Equation (2), we obtain, after some algebraic manipulation:

$$\Delta RRI(t) = \sum_{j=0}^{q_{RSA}-1} c_j^{RCC} u_j(t) + \sum_{j=0}^{q_{ABR}-1} c_j^{ABR} v_j(t) + \varepsilon_{RRI}(t) \quad (A6)$$

where $u_j(t)$ and $v_j(t)$ are new derived variables, defined as follows:

$$u_j(t) = \sum_{i=0}^{M-1} B_j^{(n)}(i) \Delta V(t-i-\tau_{RCC}) \quad (A7)$$

$$v_j(t) = \sum_{i=0}^{M-1} B_j^{(n)}(i) \Delta SBP(t-i-\tau_{ABR}) \quad (A8)$$

Equation(A6) becomes the new linear relation with unknown parameters c_j^{RCC} ($0 \leq j \leq q_{RCC}$) and c_j^{ABR} ($0 \leq j \leq q_{ABR}$) that can be estimated using least-squares minimization. However, note that Equation (A6) contains far fewer unknown parameters ($q_{RCC} + q_{ABR} < 2M$) than Equation (2).

First, the least-squares minimization procedure described above was repeated for a range of values for the delays (τ_{ABR} and τ_{RCC}), the order of generalization (n from 0 to 5), and Meixner function orders (q_{ABR} and q_{RCC} from 4 to 8). For each combination of delays, the order of generalization, and Meixner function orders, a metric of the quality of fit, known as the “minimum description length” (*MDL*), was computed (22). *MDL* was computed as follows:

$$MDL = \log(J_R) + \frac{\text{total number of parameters} \times \log(M)}{M} \quad (A9)$$

where J_R is the variance of the residual errors between the measured data and the predicted output. Note that *MDL* decreases as J_R decreases but increases with increasing model order. Selection of the “optimal” candidate model was based on a global search for the minimum *MDL*; in addition, this “optimal” solution had to satisfy the condition that the cross-correlations between the residual errors and past values of the 2 inputs ($\Delta V(t)$ and $\Delta SBP(t)$) were statistically indistinguishable from zero. Once the optimal parameter values were determined, the ABR and RSA impulse responses were computed using Equations (A1) and (A2).

Finally, the recursive least squares (RLS) algorithm was used to estimate the autoregressive model coefficients at each time step. Basically, by using the RLS algorithm, the model coefficients were estimated by minimizing the residual, sum of squared error between the model prediction and the data. To make the results less sensitive to the remote past, the squared error between the model prediction and the data (e) was weighted as follows

$$J_w = \sum_{i=0}^{t-1} \lambda^i e^2(t-i) \quad (A10)$$

where λ is a forgetting factor and $0 < \lambda < 1$. The optimum λ allows an RLS algorithm that has the fastest convergence and the most robustness.

The RLS algorithm was applied to each data set multiples time for λ from 0.88 to 0.98. The λ that minimized the mean square error between the model prediction and the data was selected.

APPENDIX 2

Table of Abbreviations

Symbol/Abbreviation	Explanation
ABR	Baroreflex component of the model
AHI	Apnea-hypopnea index
BMI	Body mass index
BP	Blood pressure (arterial)
CFS	Cold face test
CID	Circulatory dynamics component of the model
DBP	Diastolic blood pressure
DER	Direct effects of respiration component of the model
$\Delta RRI(t)$	Fluctuation in RRI about the mean level at time t
$\Delta SBP(t)$	Fluctuation in SBP about the mean level at time t
$\Delta SCO(t)$	Surrogate cardiac output (ratio of SBP(t)- DBP(t) to RRI(t))
$\Delta V(t)$	Change in incremental lung volume about the mean at time t
$h_{ABR}(t)$	Impulse response function of the ABR component
$h_{RCC}(t)$	Impulse response function of the RSA component
$h_{CID}(t)$	Impulse response function of the CID component
$h_{DER}(t)$	Impulse response function of the DER component
HFP_{RRI}	High-frequency power of RRI variability
LFP_{RRI}	Low-frequency power of RRI variability
LFP_{SBP}	Low-frequency power of systolic blood pressure variability
LHR	Ratio of low-frequency power to high-frequency power of RRI variability
MDL	Minimum description length
RLS	Recursive least squares
RRI	R-R interval
RCC	Respiratory-cardiac coupling component of model
SBP	Systolic blood pressure
τ_{ABR}	Latency associated with the baroreflex component of the model
τ_{RCC}	Latency associated with the RCC component of the model
τ_{CID}	Latency associated with the CID component of the model